Crystalline Electric Field as a Probe for Long-Range Antiferromagnetic Order and Superconducting State of $CeFeAsO_{1-x}F_x$

Songxue Chi,[1] D. T. Adroja,[2] T. Guidi,[2] R. Bewley,[2] Shiliang Li,[1] Jun Zhao,[1] J. W. Lynn,[3] C. M. Brown,[3] Y. Qiu,[3,4] G. F. Chen,[5] J. L. Lou,[5] N. L. Wang,[5] and Pengcheng Dai[1,6,*]

[1]*Department of Physics and Astronomy, The University of Tennessee, Knoxville, Tennessee 37996-1200, USA*
[2]*ISIS Facility, Rutherford Appleton Laboratory, Chilton, Didcot, Oxfordshire OX11 0QX, United Kingdom*
[3]*NIST Center for Neutron Research, National Institute of Standards and Technology, Gaithersburg, Maryland 20899-6102, USA*
[4]*Department of Materials Science and Engineering, University of Maryland, College Park, Maryland 20742, USA*
[5]*Institute of Physics, Chinese Academy of Sciences, P. O. Box 603, Beijing 100080, China*
[6]*Neutron Scattering Science Division, Oak Ridge National Laboratory, Oak Ridge, Tennessee 37831-6393, USA*

(Received 31 July 2008; published 20 November 2008)

We use inelastic neutron scattering to study the crystalline electric field (CEF) excitations of Ce^{3+} in $CeFeAsO_{1-x}F_x$ ($x = 0, 0.16$). For nonsuperconducting CeFeAsO, the Ce CEF levels have three magnetic doublets in the paramagnetic state, but these doublets split into six singlets when the Fe ions order antiferromagnetically. For superconducting $CeFeAsO_{0.84}F_{0.16}$ ($T_c = 41$ K), where the static antiferromagnetic order is suppressed, the Ce CEF levels have three magnetic doublets at $\hbar\omega = 0$, 18.7, 58.4 meV at all temperatures. Careful measurements of the intrinsic linewidth Γ and the peak position of the 18.7 meV mode reveal a clear anomaly at T_c, consistent with a strong enhancement of local magnetic susceptibility $\chi''(\hbar\omega)$ below T_c. These results suggest that CEF excitations in the rare-earth oxypnictides can be used as a probe of spin dynamics in the nearby FeAs planes.

DOI: 10.1103/PhysRevLett.101.217002 PACS numbers: 74.25.Ha, 75.50.Bb, 78.70.Nx

The rare-earth (R) oxypnictides with the general formula RFeAsO (R = La, Sm, Ce, Nd, and Pr) are currently attracting much attention due to the discovery of high-transition temperature (high-T_c) superconductivity in these materials upon chemical doping [1–4]. Although superconductivity in electron-doped LaFeAsO appears at a moderate temperature of 28 K [1], replacing La with other rare-earth ions increases T_c up to 55 K [2–4], making the rare-earth oxypnictides a new class of high-T_c superconductors with critical temperatures only surpassed by high-T_c copper oxides. Since superconductivity in these rare-earth oxypnictides appears after electron doping to suppress the static antiferromagnetic (AF) order in their parent compounds [5–8], it is important to determine the influence of magnetic interactions on the superconducting properties. Compared to LaFeAsO, where Fe is the only possible ion carrying a significant magnetic moment, the rare-earth oxypnictide with unpaired $4f$ electrons such as Ce^{3+} in CeFeAsO offers a unique opportunity to study the interplay between the rare-earth and Fe magnetic ions. In particular, by using neutron scattering to study the crystal electric field (CEF) excitations of the rare earth in RFeAsO and their doped superconductors, one can determine the electronic ground state of the R ions and therefore understand the low temperature thermodynamic and magnetic properties of these materials [9,10]. Furthermore, since the R ions are situated near the superconducting FeAs layer, CEF excitations at the R sites are sensitive to the electronic properties of the FeAs layer, and can be used as a probe to study the influence of superconductivity on spin fluctuations in the FeAs plane [11–13].

In this Letter, we report inelastic neutron scattering studies of the Ce^{3+} CEF excitations in the AF ordered CeFeAsO and superconducting $CeFeAsO_{0.84}F_{0.16}$ (T_c = 41 K) [6]. For CeFeAsO, the Ce^{3+} CEF levels are composed of three magnetic doublets at $\hbar\omega = 0$, 18.63, and 67.67 meV in the paramagnetic state. When the Fe long-range AF order sets in, these doublets are split into six singlets. In the case of $CeFeAsO_{0.84}F_{0.16}$, although the three doublets are no longer split, the intrinsic linewidth Γ and the peak position of the $\hbar\omega_1 = 18.7$ meV mode show a clear anomaly below T_c. These results suggest that the linewidth and position of the CEF transitions in the rare-earth oxypnictides are sensitive to the Fe spin ordering, and can be used as a probe of the spin dynamics in the nearby FeAs planes.

Our experiments were carried out using the MERLIN chopper spectrometer at ISIS facility, Rutherford Appleton Laboratory, Didcot, UK [14], the BT4 Filter Analyzer Neutron Spectrometer (FANS) at the NIST center for neutron research (NCNR) [15], and the NG4 Disk-chopper time-of-flight spectrometer (DCS) at NCNR, Gaithersburg, Maryland. Our CeFeAsO and $CeFeAsO_{0.84}F_{0.16}$ samples were prepared using methods described in Ref. [2], and their structural or magnetic properties are discussed in Ref. [6]. For MERLIN measurements, the incident beam energies were E_i = 7, 10, 31, 73, 105, 312 meV. To separate the CEF magnetic scattering from phonons, we also measured LaFeAsO and $LaFeAsO_{0.92}F_{0.08}$ samples [5] as reference materials for phonon subtraction from the Ce samples. The La samples did not reveal any clear change in phonon spectra below and above T_c, hence allowed us to

use these samples to subtract the phonons in the Ce samples. The data for $CeFeAsO_{1-x}F_x$ and $LaFeAsO_{1-x}F_x$ were converted to absolute units of mb/sr/meV/f.u. by normalizing the scattering to a vanadium standard. For the DCS measurements, we used an incident beam energy of 3.55 meV.

Figure 1(a) shows the position of the Ce ion in the crystal structure environment of CeFeAsO. Relative to the Fe sublattice, the Ce^{3+} ions are located alternately above and below the (AF ordered) Fe layers as shown in Fig. 1(b). Figs. 1(c) and 1(d) summarize the Ce CEF excitation energies determined from our inelastic neutron scattering experiments for CeFeAsO and $CeFeAsO_{0.84}F_{0.16}$, respectively. According to neutron powder diffraction experiments [6], both CeFeAsO and $CeFeAsO_{0.84}F_{0.16}$ have a tetragonal (space group $P4/nmm$) crystal structure at room temperature. However, on cooling, CeFeAsO first exhibits a structural phase transition, changing the crystal symmetry from tetragonal to orthorhombic (space group $Cmma$), and then orders antiferromagnetically with a spin structure as shown in Figs. 1(a) and 1(b) [5,6]; $CeFeAsO_{0.84}F_{0.16}$ maintains the tetragonal structure and does not order magnetically above 4 K. In the tetragonal structure, the Ce atoms are located at the $2c$ crystallographic site which has C_{4v} point symmetry. This gives three nonzero CEF parameters in the crystal field Hamiltonian, and its form in Stevens operators formalism is $H_{\mathrm{CEF}}(C_{4v}) = B_2^0O_2^0 + B_4^0O_4^0 + B_4^4O_4^4$. In the case of the low-T orthorhombic structure of CeFeAsO, the Ce atoms are at the $4g$ (0, 1/4, z) site which gives local point symmetry of $mm2$ (C_{2v}). The resulting Hamiltonian then involves five nonzero crystal field parameters as $H_{\mathrm{CEF}}(C_{2v}) = B_2^0O_2^0 + B_2^2O_2^2 + B_4^0O_4^0 + B_4^2O_4^2 + B_4^4O_4^4$, where B_n^m's are the CEF parameters to be determined from the experimental data, and O_n^m's are operator equivalents obtained using the angular momentum operators [9].

We collected neutron scattering data on CeFeAsO and $CeFeAsO_{0.84}F_{0.16}$ on MERLIN and DCS spectrometers with different incident beam energies to search for Ce^{3+} CEF excitations. To eliminate phonon scattering, we carried out identical scans using LaFeAsO and $LaFeAsO_{0.92}F_{0.08}$ as reference materials. Figs. 2(a) and 2(b) show the phonon subtracted energy scans for CeFeAsO at 7 K and 200 K on MERLIN obtained with $E_i = 30.8$ meV and $E_i = 105$ meV. The inset of Fig. 2(a) plots similar data taken on DCS with $E_i = 3.55$ meV. Identical scans taken for $CeFeAsO_{0.84}F_{0.16}$ are shown in Figs. 2(c) and 2(d). We first discuss results on the superconducting sample as there are no complications of structural distortion and Fe magnetic order. To obtain the B_n^m's CEF parameters in the $H_{\mathrm{CEF}}(C_{4v})$ Hamiltonian, we first used the FOCUS program, which has a Monte Carlo search

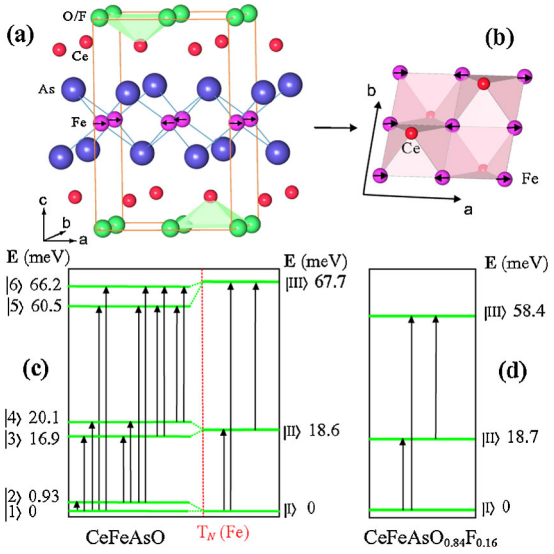

FIG. 1 (color online). Summary of the CeFeAsO crystal or magnetic structure and CEF levels determined from our inelastic neutron scattering experiments. (a) The Fe spin ordering in the CeFeAsO chemical unit cell. (b) The Fe spins in CeFeAsO with respect to the Ce positions. The Fe moments lie in the a-b plane along the a axis and form an antiferromagnetic collinear spin structure. (c) Ce^{3+} CEF levels in CeFeAsO for temperatures above and below the Fe AF Néel temperature of $T_N = 140$ K [6]. The arrows indicate possible transitions. (d) Ce^{3+} CEF levels in superconducting $CeFeAsO_{0.84}F_{0.16}$ at low temperature.

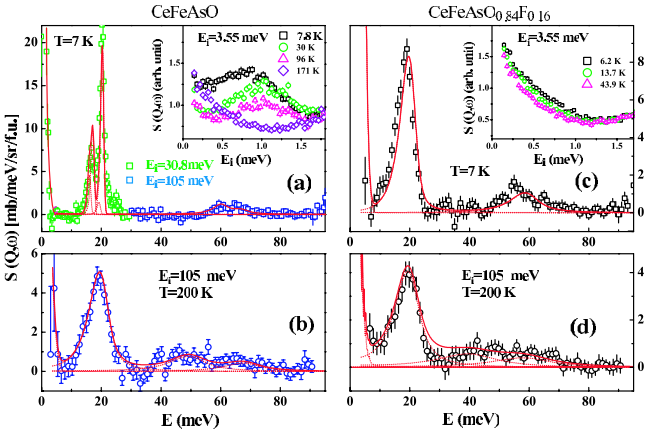

FIG. 2 (color online). Temperature dependence of the CEF excitations in CeFeAsO and $CeFeAsO_{0.84}F_{0.16}$ integrated over $0 < Q < 4$ Å^{-1} and our model determination of the CEF levels. (a) Ce CEF magnetic excitations in absolute units after subtracting the LaFeAsO phonons. The squares to the left denote the data with $E_i = 30.8$ meV to show the splitting. The solid line is our model fit with parameters listed in Table I. The inset shows the raw DCS data integrated over $0 < Q < 2.2$ Å^{-1} in arbitrary units as a function of temperature without the LaFeAsO phonon subtraction. (b) Ce CEF excitations at 200 K; solid line is our model calculation. (c–d) CEF excitations and their temperature dependence for $CeFeAsO_{0.84}F_{0.16}$. The solid lines are model calculations. Inset in (c) shows that the 0.7 meV excitation seen in CeFeAsO is missing in $CeFeAsO_{0.84}F_{0.16}$. Error bars represent 1 standard deviation.

TABLE I. Refined B_n^m CEF parameters for CeFeAsO and $CeFeAsO_{0.84}F_{0.16}$.

	$CeFeAsO_{0.84}F_{0.16}$	CeFeAsO ($>T_N$)	CeFeAsO ($<T_N$)
B_2^0	2.545 ± 0.089	3.155 ± 0.120	3.012 ± 0.102
B_4^0	−0.045 ± 0.005	−0.029 ± 0.007	0.031 ± 0.002
B_2^2			1.972 ± 0.365
B_4^2			−0.061 ± 0.045
B_4^4	0.641 ± 0.026	0.710 ± 0.044	0.440 ± 0.041

routine, to fit the observed two CEF excitations at 18.7 meV and 58.4 meV in Figs. 2(c). We then fit many spectra simultaneously with different incident energies and temperatures using a CEF fit program, and the results are plotted as solid lines in Figs. 2(c) and 2(d) for 7 and 200 K, respectively. Tables I and II summarize the B_n^m's CEF parameters and wave functions for $CeFeAsO_{0.84}F_{0.16}$ obtained from those fits.

Comparing to the superconducting $CeFeAsO_{0.84}F_{0.16}$, the Ce CEF excitations in CeFeAsO near 19 and 65 meV have clear double peaks at low temperature that become a single peak at 200 K [Figs. 2(a) and 2(b)]. In addition, the low-energy spectra in the inset of Fig. 2(a) show a clear peak around 0.9 meV that is not present at 171 K. To understand this phenomenon, we carried out careful temperature dependence measurements of the ~19 meV CEF excitation. Figure 3(a) shows the raw $S(Q, \omega)$ spectra of CeFeAsO collected on MERLIN at 60 K using $E_i = 30.8$ meV. After subtracting the phonon scattering background collected using LaFeAsO, the Ce CEF level shows two clear bands of excitations at 16.9 and 20.1 meV [Fig. 3(b)]. Figure 3(c) shows the detailed temperature dependence of the ~19 meV excitations and Fig. 3(d) plots the splitting of the two low temperature peaks. Comparison of these figures with the Néel temperature of CeFeAsO in Fig. 3(e) makes it clear that the CEF splitting is due to the long-range AF Fe ordering [6].

In principle, the orthorhombic structural distortion that precedes the AF ordering in CeFeAsO can have an effect on the Ce CEF levels. However, since neutron powder diffraction data [6] showed that the Ce local environment is not much affected by the lattice distortion, we started fitting the low temperature spectra using the CEF parameters for tetragonal geometry, then added the effect of the molecular field of the Fe spins in the presence of the orthorhombic structural distortion. The solid line in Fig. 2(a) shows our fit to the data, and the CEF parameters for temperatures above and below T_N are also given in Table I. Although the splittings of the doublets and their transition intensities can be reproduced using orthorhombic point symmetry with molecular field $H_x = H_z = 1.129 \pm 0.13$ meV, the CEF parameters for $T < T_N$ are not unique. Since Ce ions reside at the center of Fe squares, a molecular field on the Ce site is not expected unless Fe ions have additional anisotropic interactions such as Fe-Ce exchange coupling. Assuming that the $|\mathrm{I}\rangle$, $|\mathrm{II}\rangle$, and $|\mathrm{III}\rangle$ doublets in the paramagnetic state of CeFeAsO split into $|1\rangle$ to $|6\rangle$ singlets in the AF state as shown in Fig. 1(c), the observed excitations near 19 meV should be composed of 4 possible transitions $|1\rangle \rightarrow |3\rangle$, $|1\rangle \rightarrow |4\rangle$, $|2\rangle \rightarrow |3\rangle$, and $|2\rangle \rightarrow |4\rangle$. Since the transition probabilities $|\langle 1|J_z|3\rangle|^2$ and $|\langle 2|J_z|4\rangle|^2$ are rather small, the observed excitations at 16.9 and 20.4 meV in Fig. 2(a) actually arise from $|1\rangle \rightarrow |4\rangle$ and $|2\rangle \rightarrow |3\rangle$, and are controlled by the thermal population of $|1\rangle$ and $|2\rangle$, respectively. This is consistent with the temperature dependence of these two excitations, where the 16.9 mode decreases and the 20.1 meV excitation increases with decreasing temperature [Fig. 3(c)].

In rare-earth substituted high-T_c copper oxides such as $Tm_{0.1}Y_{0.9}Ba_2Cu_3O_{6+x}$ [11] and $Ho_{0.1}Y_{0.9}Ba_2Cu_3O_7$ [12],

TABLE II. Wave functions of different CEF levels for $CeFeAsO_{0.84}F_{0.16}$ and CeFeAsO above T_N.

	$CeFeAsO_{0.84}F_{0.16}$	CeFeAsO ($>T_N$)
$\|\mathrm{I}\rangle$	$\|\mp 1/2\rangle$	$\|\mp 1/2\rangle$
$\|\mathrm{II}\rangle$	$-0.5\|\mp\frac{5}{2}\rangle + 0.866\|\pm\frac{3}{2}\rangle$	$-0.43\|\mp\frac{5}{2}\rangle + 0.902\|\pm\frac{3}{2}\rangle$
$\|\mathrm{III}\rangle$	$0.866\|\mp\frac{5}{2}\rangle + 0.5\|\pm\frac{3}{2}\rangle$	$0.902\|\mp\frac{5}{2}\rangle + 0.43\|\pm\frac{3}{2}\rangle$

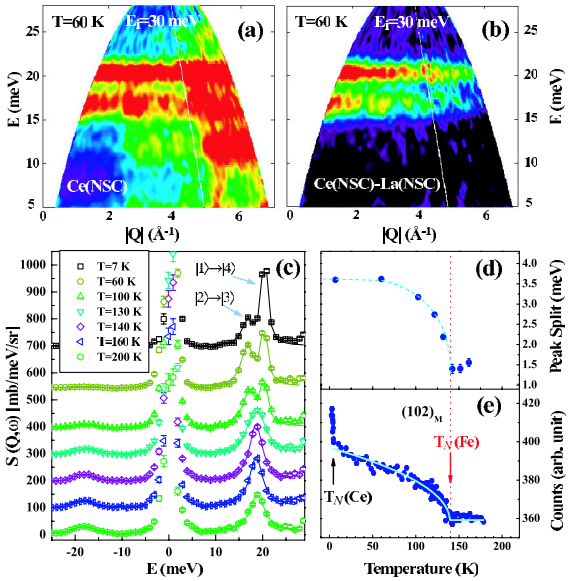

FIG. 3 (color online). (a) Raw $S(Q, \omega)$ spectra of CeFeAsO at 60 K and $E_i = 30$ meV on MERLIN. (b) Ce CEF excitations after subtraction of the LaFeAsO background. (c) Temperature dependence of the 18.7 meV excitations. The peaks around 18 meV at 7 K are fitted with 2 Lorentzians, the widths of which were fixed for fittings at all higher temperatures. Although this ignores the broadening of linewidths upon warming and gives illusionary finite peak separation above T_N, the net splitting solely caused by molecular field can be monitored by abrupt change of this separation which happens below 140 K, the T_N of Fe as shown in (e).

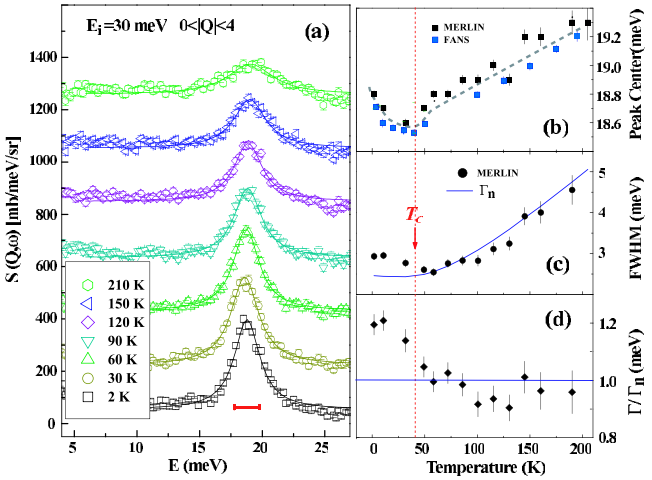

FIG. 4 (color online). Temperature dependence of the $\hbar\omega_1 = 18.7$ meV Ce CEF excitation for $CeFeAsO_{0.84}F_{0.16}$. (a) MERLIN measurements using $E_i = 30.8$ meV at different temperatures. The instrumental energy resolution is 2.1 meV at elastic position (horizontal bar). (b) The peak position as a function of temperature for the 18.7 meV CEF level. The solid squares are MERLIN data while light squares are FANS data; both show a clear anomaly at T_c. (c) The intrinsic linewidth $\Gamma(T)$ as a function of temperature. The solid line shows the expected $\Gamma_n(T)$ assuming noninteracting Fermi liquid. $\Gamma(T)$ deviates from $\Gamma_n(T)$ near T_c. (d) $\Gamma(T)/\Gamma_n(T)$ shows a clear anomaly near T_c, consistent with (c).

the intrinsic linewidth Γ and peak position of the rare-earth CEF excitations are used to probe the local magnetic response of the CuO_2 planes and the formation of a superconducting energy gap. The CEF excitations of Ho and Er have also been used to study pseudogap and order-parameter symmetry in the underdoped superconducting $HoBa_2Cu_4O_8$ and $Er_2Ba_4Cu_7O_{14.92}$, respectively [13]. To see if the $\hbar\omega_1 = 18.7$ meV CEF excitation in $CeFeAsO_{0.84}F_{0.16}$ is also sensitive to the occurrence of superconductivity, we carefully probed the temperature dependence of its intrinsic linewidth Γ [Figs. 4(a) and 4(c)] and peak position [Fig. 4(b)]. Figure 4(a) shows the phonon subtracted data at different temperatures. Figure 4(b) plots the peak position as a function of temperature, which shows a clear anomaly around T_c. Inspection of Fig. 4(c) reveals that the linewidth decreases with decreasing temperature. For the case when the CEF levels do not overlap, the temperature dependence of the linewidth $\Gamma(T)$ of the transition between the ground state ($|1\rangle$) and the first excited state ($|2\rangle$) in Fig. 1(c) can be accurately estimated using Eq. 1 in [12]. To first order, this can be written as $\Gamma(T) \propto \chi''(\hbar\omega_1)\coth(\frac{\hbar\omega_1}{2k_BT})$, where $\chi''(\hbar\omega_1)$ is the local integrated magnetic susceptibility at $\hbar\omega_1 (= 18.7$ meV) and k_B is the Boltzmann constant [11].

To understand $\Gamma(T)$, we calculate the linewidth $\Gamma_n(T)$ below 150 K using this equation assuming a noninteracting Fermi liquid normal state [12], even though this is still under discussion. The solid line in Fig. 4(c) shows the outcome of our calculation. The observed linewidth starts to deviate from the expected values near T_c, as shown more clearly in $\Gamma(T)/\Gamma_n(T)$ [Fig. 4(d)]. The most natural interpretation of Figs. 4(c) and 4(d) is that the local integrated magnetic susceptibility $\chi''(\hbar\omega_1)$ from the Fe spin fluctuations at 18.7 meV increases dramatically below T_c. Since the temperature dependence of this excitation and its energy are rather similar to that of the neutron spin resonance recently observed in $Ba_{0.6}K_{0.4}Fe_2As_2$ [16], we speculate that the observed linewidth change might be related to the spin resonance in $CeFeAsO_{0.84}F_{0.16}$.

In summary, we have determined the Ce CEF levels in nonsuperconducting CeFeAsO and superconducting $CeFeAsO_{0.84}F_{0.16}$ as a function of temperature. Our results show that Ce CEF excitations are very sensitive to the Fe magnetic order in the undoped system, and dynamic spin susceptibility in the superconductor, and therefore can be used as a probe to study spin dynamical properties of the rare-earth based oxypnictides.

We thank B. D. Rainford, T. Yildirim for discussions and E. Goremychkin and R. Osborn for providing the CEF program. This work is supported by the US DOE BES through No. DE-FG02-05ER46202, and in part by the US DOE, Division of Scientific User Facilities. DCS is supported by NSF No. DMR-0454672. The work at the IOP, CAS, is supported by the NSF of China, the CAS, and the Ministry of Science and Technology of China.

*daip@ornl.gov

[1] Y. Kamihara *et al.*, J. Am. Chem. Soc. **130**, 3296 (2008).
[2] X. H. Chen *et al.*, Nature (London) **453**, 761 (2008).
[3] G. F. Chen *et al.*, Phys. Rev. Lett. **100**, 247002 (2008).
[4] Zhi-An Ren *et al.*, Europhys. Lett. **83**, 17 002 (2008).
[5] C. de la Cruz *et al.*, Nature (London) **453**, 899 (2008).
[6] J. Zhao *et al.*, Nature Mater. (to be published).
[7] M. A. McGuire *et al.*, Phys. Rev. B **78**, 094517 (2008).
[8] Q. Huang *et al.*, Phys. Rev. B **78**, 054529 (2008).
[9] P. Fulde and M. Loewenhaupt, Adv. Phys. **34**, 589 (1985).
[10] J. Mesot *et al.*, J. Supercond. **10**, 623 (1997).
[11] R. Osborn and E. A. Goremychkin, Physica (Amsterdam) **185–189C**, 1179 (1991).
[12] A. T. Boothroyd *et al.*, Phys. Rev. Lett. **77**, 1600 (1996).
[13] J. Mesot *et al.*, Europhys. Lett. **44**, 498 (1998).
[14] R. Bewley *et al.*, Physica (Amsterdam) **385–386B**, 1029 (2006).
[15] T. J. Udovic *et al.*, Nucl. Instrum. Methods Phys. Res., Sect. A **517**, 189 (2004).
[16] A. D. Christianson *et al.*, arXiv.org/abs/0807.3932.